

Thermal Analysis of Automobile Radiator with Honeycomb Fins

Md. Khalid¹, Dr. Sohail Bux²

¹M.Tech Scholar, Department of Mechanical Engineering, Agnos College of Technology, RKDF University, Bhopal (M.P.)

²HOD, Department of Mechanical Engineering, Agnos College of Technology, RKDF University, Bhopal (M.P.)

Email: khalidqusba@gmail.com, buxsohail@gmail.com

* Corresponding Author: Md. Khalid

Abstract: This research paper investigates the relationship between mass flow rate and the length of the fully developed velocity region in a tube. It examines the impact of velocity profile on heat transfer rates and analyzes the correlation between heat transfer coefficient and the length of the fully developed temperature region in a radiator with honeycomb fins. The study also explores the influence of pressure drop on temperature drop and compares the pressure and temperature drops for different heat transfer values. Additionally, the effect of flow rate on coolant temperature drop and the relationship between cross-sectional area, laminar flow, and heat transfer in tubes are investigated. The findings suggest that higher flow rates decrease the coolant's temperature drop, while laminar flow and small tube cross-sectional areas indirectly decrease heat transfer.

Keywords: Cooling system, air cooling, conduction, convection, thermal efficiency.

1. INTRODUCTION

An energy crisis was caused by an excessive and alarming rate of use of conventional fossil fuels, which also contributed to environmental issues like ozone depletion, greenhouse gas emissions, and global warming that endanger human security and the future of the planet [1]. In order to lessen our reliance on fossil fuels and address the negative environmental effects that follow, there is a greater need for clean energy technology. Due to its cleanliness, ease of accessibility, sustainability, and limitless potential, solar energy is the most widely used and well acknowledged renewable energy source [2].

As the manufacturing process for integrated circuits is being improved, more heat is being produced. The integrated circuit industry therefore requires effective heat management technologies, which are anticipated to continue enhancing the functionality and dependability of electronic products. For certain conventional electronic devices, traditional air cooling may manage the heat dissipation difficulties by improving the heat sink design [3], but additional alternative cooling strategies are urgently required for sophisticated high-performance electronic devices. Heat transmission is the basis for how the cooling system operates. Always, heat will go from a hotter to a colder thing. There are three different ways to transmit heat: conduction, convection, and radiation. Convection is the transmission of heat by the circulation of heated parts of a liquid gas; convection is defined as the transfer of heat by the circulation of heated parts of a liquid gas. Convection is used to transmit heat from the hot cylinder block to the coolant. When the heated radiator parts transfer heat to the coolant air surrounding the radiator, this is known as convection.

Heat can also be delivered by radiation. Radiation is defined as the process of transferring heat by converting it to radiant energy. Radiation is emitted by any heated item. The more radiant energy a thing emits, the hotter it is. Some of the heat generated by the engine is transferred to radiant heat (about 9 percent). These concepts are used by the cooling system to remove excess heat from the engine. Heat transfer enhancement is an ever-lasting topic for various thermal applications, such as heat exchangers, electronic cooling, heat reservoirs, solar collectors, cooling of nuclear reactors, and so on. The thermal performance of heat transfer equipment may be significantly enhanced by using porous metals with high solid thermal conductivities as a unique type of ideal heat transfer material [4].

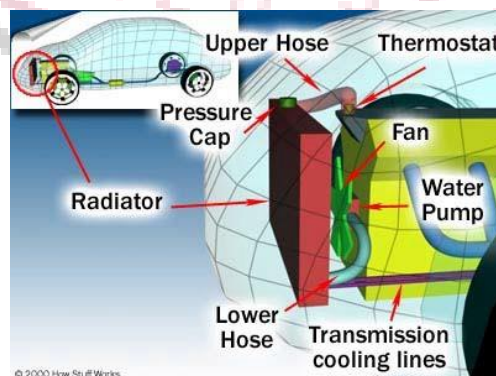


Figure 1 Cooling System

The turbocharger has been built as a high-tech product integrating mechanical, electrical, new materials, and other disciplines [7], and it serves as a major auxiliary component of the engine [5], which typically functions in hostile environments. The operating performance of the engine will be enhanced and the exhaust emissions will be lowered [10] whether the turbocharger is paired with a diesel engine, gasoline engine, or even a hybrid electric vehicle [8–9]. In recent years, turbocharger technology has been adopted to meet the more stringent engine pollution laws [11]. The use of turbochargers is expanding at this time, which encourages engine downsizing and improves engine efficiency and environmental friendliness [12].

Engine manufacturers today commonly used two types of cooling system: Air cooled system and Liquid cooled system. Air-cooled engines have been designed by a number of manufacturers. Air-cooled engines are still used by several international manufacturers. Fins or ribs cover the exterior surfaces of the cylinder and cylinder heads in air-cooled engines. These fins are attached to the cylinder and heads directly. The fins enhance the object's surface area, which increases the amount of available convection and radiation for heat transfer. The heat generated by combustion is transferred to the outer fins by conduction from the engine's interior elements. The heat is dissipated in this area to the passing air. Individual cylinders are sometimes utilised to improve air circulation around the cylinder. Air must circulate around the cylinder block and heads in air-cooled engines. To move the air across the engine, a fan is frequently utilised. A shroud is also utilised to direct or control the flow of air across the engine in some circumstances. Air-cooled engines do not have precise temperature control, but they do not require a radiator or a water pump. Over time, this may result in lower engine maintenance costs.

The heat from the cylinder is transferred to a liquid flowing through jackets around the cylinders in a liquid cooled engine. After that, the liquid passes via a radiator. The heat from the liquid is transferred to the air by air moving through the radiator. Temperature control is usually greater with liquid cooling systems than with air cooling systems. They're made to keep coolant temperatures between 820 and 980 degrees Celsius. When the coolant temperature is at 200 degrees Fahrenheit, the engine runs best (93 degrees Celsius). The coolant travels from the thermostat to the radiator's internal tubes. In the core, there are tubes with little fins on them. The air going through the radiator is now cooling the coolant. It then makes its way back to the pump via the radiator output. It continues to circulate through the engine after that.

In this work, a laminar flow regime ($100 > Re > 1000$) is used to experimentally analyze the total heat transfer coefficient of CuO/water nanofluids in a vehicle radiator. The overall heat transfer coefficient falls when the nano fluid inlet temperature increases from 50°C to 80°C. The total heat transfer coefficient is increased by up to 8% when nanofluid is added compared to the base fluid. The total heat transfer coefficient using nanofluid as a function of nanofluid flow rate and nanoparticle concentration at a fixed air flow rate. It is shown that when the flow rate of the nanofluid rises, the total heat transfer coefficient increases significantly. For big particles, for example, at an air flow rate of 870m³/h, a nanofluid concentration of 0.4 vol. percent, and a nanofluid inlet temperature of 80°C. CFD simulation is used to determine the highest value of the overall heat transfer coefficient using nanofluid, the effect of each operating parameter on the overall heat transfer coefficient, and the optimum values of each parameter.

The primary objective of this study is to determine the relationship between the mass flow rate and the length of the fully developed velocity region in a tube. Additionally, the investigation aims to assess the impact of the velocity profile on heat transfer rates, particularly at 400 or 300 W/m².K. Another objective is to examine the relationship between the heat transfer coefficient and the length of the fully developed temperature region in a radiator equipped with honeycomb fins. Furthermore, the analysis seeks to analyze the influence of pressure drop on temperature drop for different values of heat transfer. Additionally, a comparative analysis of the pressure drop and temperature drop for various heat transfer values will be conducted to assess their similarities. The study also aims to investigate the effect of flow rate on the temperature drop of coolant, considering the potential impact of utilizing different cross-sectional tube shapes. Finally, the objective is to study the relationship between the cross-sectional area, laminar flow, and heat transfer in tubes.

II. LITERATURE REVIEW

According to (Gonçalves, I. et. al., 2021) [13] In recent years, the nanofluids (NFs) have become the main candidates for improving or even replacing traditional heat transfer fluids. The utilization of NFs in numerous technical applications, from nanomedicine to renewable energy, has made NFs and their thermal conductivity one of the most researched issues in the present day. Therefore, this study provides a summary of the most significant developments and contentious findings in relation to the NFs thermal conductivity. It is detailed how to test the thermal conductivity of NFs using several methods. Additionally, the basic factors that influence the NFs thermal conductivity are examined, and potential advancements including a rise in the nanoparticles' (NPs) long-term stability are discussed. On the basis of fluid mechanics, thermodynamics, and experimental fits, the most typical classical prediction models are provided. Also, the recent statistical machine learning-based prediction models are comprehensively addressed, and the comparison with the classical empirical ones is made, whenever possible.

(Sekrani, G., & Poncet, S, 2018) [14] investigated that Nanofluids are considered a promising way to improve the heat transfer capability of base fluids. Water is the most commonly-used heat transfer fluid. However, in refrigeration systems, it may be necessary to mix water with either ethylene- or propylene-glycol to lower its freezing point and prevent from ice formation. In the same way, for car radiators or industrial heat exchangers, the boiling point of water can be pushed up by mixing it with glycol-based fluids. The increasing awareness of energy saving and industrial energy efficiency improvement results in the growing interest in ethylene- or propylene-glycol-based nanofluids for applications in various

thermal systems. The present paper proposes an extensive review of the most recent and relevant experimental and numerical works on the thermophysical properties and performances of ethylene- or propylene-glycol-based nanofluids. Research perspectives are also provided with the long-term objective that these nanofluids be more widely considered in real industrial applications.

(S.C. Pang, et al., 2012) [15] Engine cooling system plays an important role to maintain the operating temperature of engine. The coolant circuit initiates by picking up heat at water jackets. When the coolant circuit has a pressure gradient, hot coolant flows out of the engine and into the radiator or a bypass circuit (during a cold start). After passing through various hood components, the under-hood air flow transfers heat to the radiator. At the radiator, the coolant flow circuit and the air flow circuit converge and exchange heat. The cooling system of cars is the subject of substantial research, both mathematically and experimentally. The study examines a wide range of specialized subjects, including the after-boiling phenomena of coolants, under-hood air flow, heat transfer at water jackets and radiators, and numerical modeling of engine cooling systems.

III. METHODOLOGY

For many years, computational fluid dynamics (CFD) has been a strong approach for studying heat and mass transfer. CFD codes are built around numerical techniques that can be used to solve fluid flow issues. In a discretized form, CFD provides numerical solutions to partial differential equations governing airflow and heat transfer. CFD software can study the sophisticated fluid flow and heat transfer processes involved in any heat exchanger.

The temperature of the water inflow is the same as the engine's temperature. The entire theoretical procedure starts with Equation 1 for the radiator's heat transmission rate. The only two unknowns for the system are the air and water outlet temperatures, as shown in this equation. These two unknowns are assumed at first. The following equations and formulas are used to simply solve for both outlet temperatures. The iteration of the initially assumed and computed outlet temperatures is used to get the real values for the air and water outlet temperatures.

$$q = m_{air}c_{p,air}(T_{air,out} - T_{air,in}) = m_{water}c_{p,water}(T_{water,in} - T_{water,out})$$

Internal Flow of Water

The hot water from the engine travels through the tubes of the radiator.

Area of Tubes

$$D_{hydraulic} = \frac{4A_{tube}}{P_{tube}}$$

Reynolds Number

$$Re_{water} = \frac{\rho_{water}v_{water}D_{hydraulic}}{\mu_{water}}$$

Nusselt Number

For fully developed laminar flow, the Nusselt number was calculated as a constant in Table 8.1 for a rectangular cross section. In this table, the Nusselt number is calculated by dividing the tube's diameter by its height. As a result, the Nusselt number is 3.96. Water Flow Convective Heat Transfer Coefficient

$$h_{water} = \frac{Nu_{water}k_{water}}{D_{hydraulic}}$$

Mean Temperature of Air

To determine the necessary material qualities for later usage, the average temperature of air must be estimated. Specific heat, thermal conductivity, kinematic viscosity, and Prandtl number are the qualities in question.

Velocity

$$v_{air} = \frac{Q_{air}}{A_{radiator} - (N_{tube}H_{tube}L_{radiator})}$$

Reynolds Number

$$Re_{air} = \frac{v_{air}W_{fin}}{\nu_{air}}$$

Nusselt Number

Looking at the geometry of the tubes, it can be assumed that the flow of air is similar to parallel flow over a flat plate. Since the flow never reaches the critical Reynolds number for a flat plate, $Re = 5 \times 10^5$, it is said to be laminar for the entire process.

$$Nu_{air} = .664Re_{air}^{1/2}Pr_{air}^{1/3}$$

Convective Heat Transfer Coefficient for Air Flow

Overall Surface Efficiency

The overall surface efficiency is needed for the external flow of air because the imperfections of the flow around the fins must be considered.

$$\eta_o = 1 - \frac{N_{fin} A_F}{A_{fin,base}} (1 - \eta_{fin})$$

Effectiveness-NTU Method

The efficacy of the system is determined using the Effectiveness-NTU approach. It is necessary to calculate the entire heat transfer coefficient. Because the defects of the flow surrounding the fins must be considered, the surface efficiency is required for the external flow of air. The UA is determined using the convective heat transfer coefficients of both the internal and exterior flows. The NTU is then calculated using this value.

Overall Heat Transfer Coefficient

$$UA = \frac{1}{\left(\frac{1}{\eta_o h_{air} A_{external}} + \frac{1}{h_{water} A_{internal}} \right)}$$

Number of Transfer Units

$$NTU = \frac{UA}{C_{min}}$$

Effectiveness

The radiator utilizes a cross-flow single pass design where both fluids remain unmixed. This correlates to a specific equation to calculate effectiveness. However, this equation requires the heat capacity ratio, Cr, to be equal to 1. The calculated heat capacity ratio is 0.455; therefore, the effectiveness is only a close approximation instead of the true value.

Heat Transfer Rate

To determine the projected heat transfer rate, the maximum heat transfer rate must be determined. Once this is known, a modified version of the beginning thermal energy calculation is used to calculate the final output temperature of both the hot and cold fluids. These outlet temperatures must be compared to the originally estimated outlet temperatures until they are equal. The theoretical values for both air and water iterated output temperatures are utilised to compare with the experimental results.

$$\varepsilon = 1 - \exp \left[\left(\frac{1}{C_r} NTU^{0.22} \right) \left(\exp(-C_r NTU^{0.78}) - 1 \right) \right]$$

Max heat transfer rate

$$q_{max} = C_{min} (T_{water,in} - T_{air,in})$$

Predicted Heat Transfer

$$q_{predicted} = \varepsilon q_{max}$$

Temperature Out

$$T_{water,out} = T_{water,in} - \frac{q_{predicted}}{C_{water}}$$

$$T_{air,out} = T_{air,in} - \frac{q_{predicted}}{C_{air}}$$

IV. RESULTS

From an engineering standpoint, simulation is a widely used and rather ill-defined phrase. "To simulate" implies "to feign, to obtain the essence without the reality," according to Webster's international dictionary. The most basic definition of simulation is "imitation." For engineering applications, these dictionary definitions don't paint a clear picture of the word "Simulation." As a result, a definition of the term "Simulation" would be more accurate in this situation. The author defines simulation as follows, with considerable trepidation:

"The act of constructing a model of a real system and conducting experiments with it in order to understand the behaviour of the system is known as simulation."

Meshing

Meshing in CFD is a large topic. This post will be the first of a multi-post series addressing the topic. The stages of meshing in CFD are:

1. Basic Mesh
2. Initial Mesh
3. Solution-Adaptive Mesh

The first mesh created was Basic Mesh. Most of the time, it divides the computational domain into cells of identical size, ignoring model geometry. When utilising manual settings, the user commonly enters the number of cells in the x-, y-, and

z-directions to calculate the overall number of 3D grid starting cells. In this piece, I'll go over the basic mesh and its settings after addressing the processes of meshing in the first part of this series.

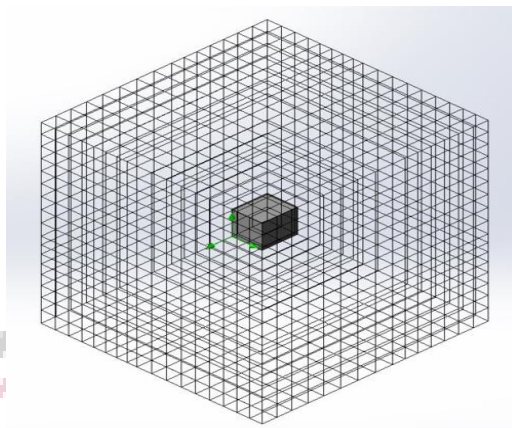


Figure 2 Basic Mesh of a cube

The analysis tool SOLIDWORKS flow simulation is used to perform CFD analysis on radiator. By observing the analysis results, with above configuration solution results of the modified model are converged than the original that is the radiator with 16 Honeycomb fins and 54 fins. There are 4 design points in the parametric study and all these are same for all the cases. In first four mass flowrate along x-axis design points varies as 0.1, 0.2, 0.3 and 0.4 kg/s and other is heat transfer rate varies as 400 W/m².K and 300 W/m².K. Results of these parametric studies are as follows,

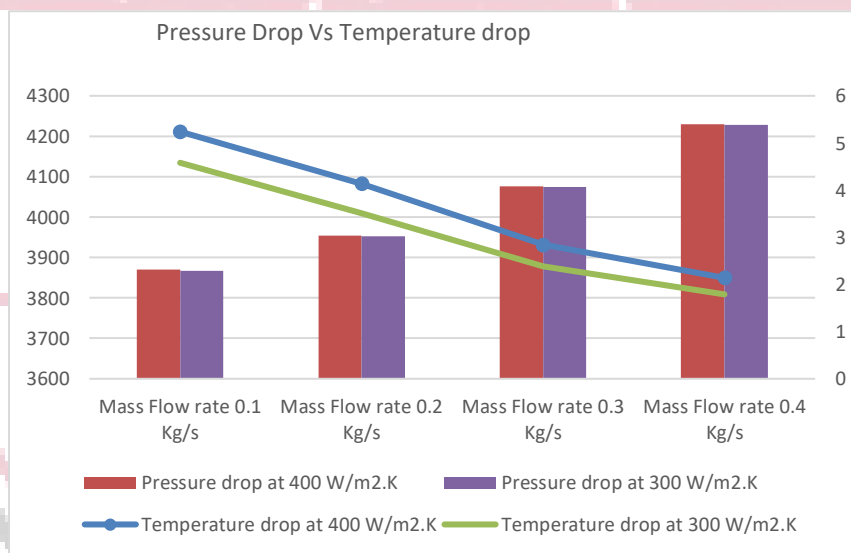


Figure 3 Graph of pressure drop vs temperature drop at 400 and 300 W/m².K

All the results are converged after 950 iterations. Parameters of the goals with average value are given in the table. Temperature flow trajectory, Pressure flow trajectory and the velocity flow trajectory cut plots along the front, top and right planes of the turbine is taken. Pressure counter gives how the pressure varies along the turbine and along down stream of air velocity counter along with the vector directions are also plot of the same planes and temperature plot respectively.

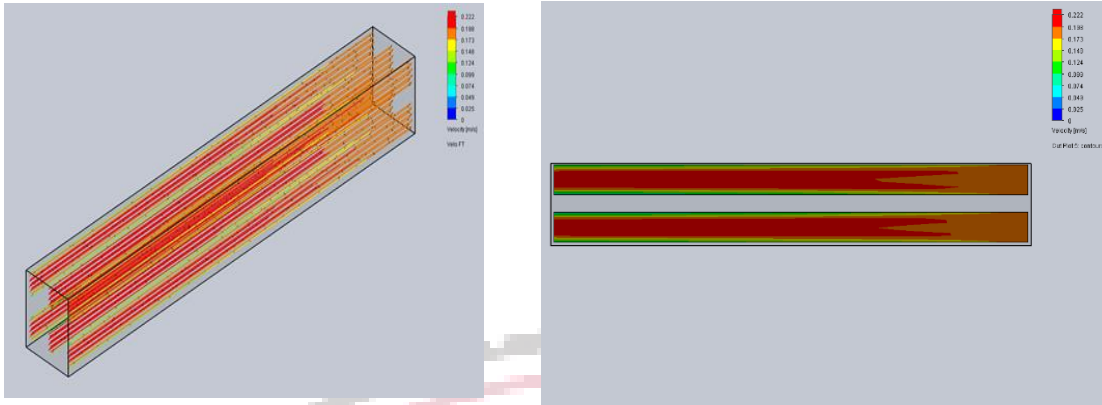


Figure 4 Velocity flow trajectory and cutplot along the radiator $m= 0.1$ kg/s

Velocity flow trajectory and Cut plot of radiator at 400 W/m².K

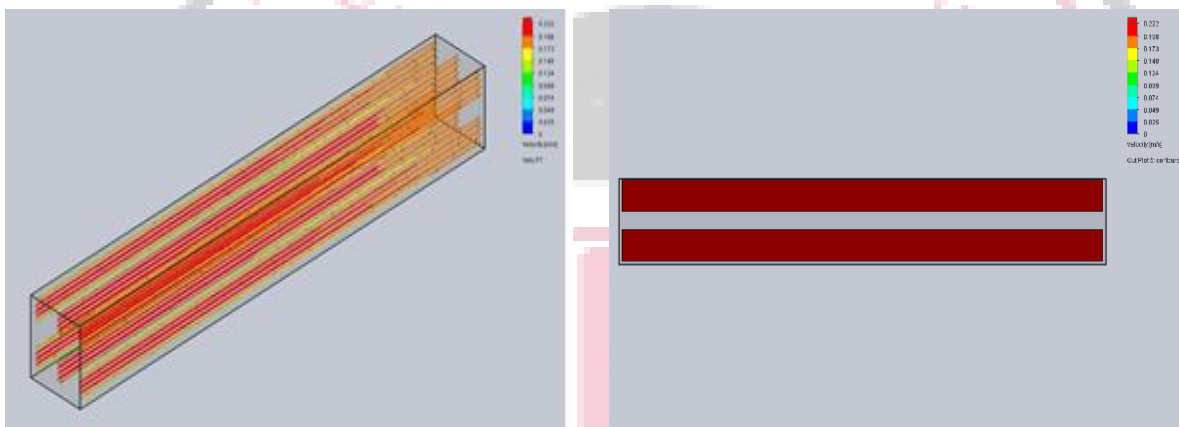


Figure 5 Velocity flow trajectory and cutplot along the radiator $m= 0.2$ kg/s

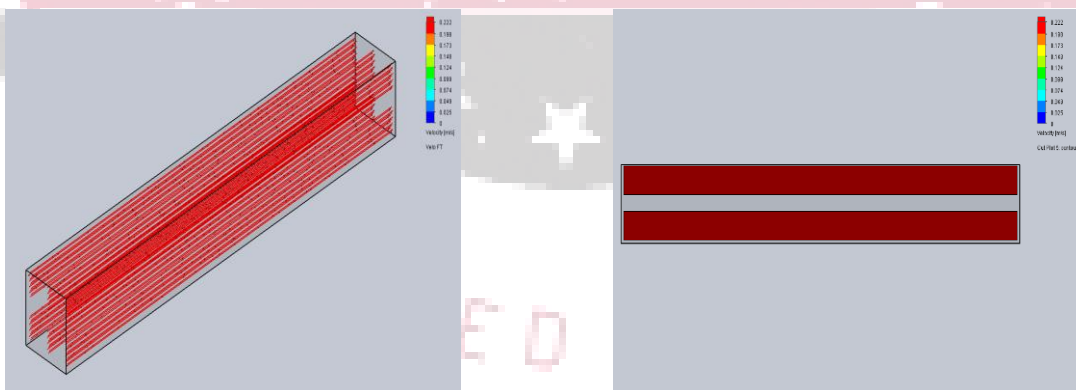


Figure 6 Velocity flow trajectory and cutplot along the radiator $m= 0.3$ kg/s

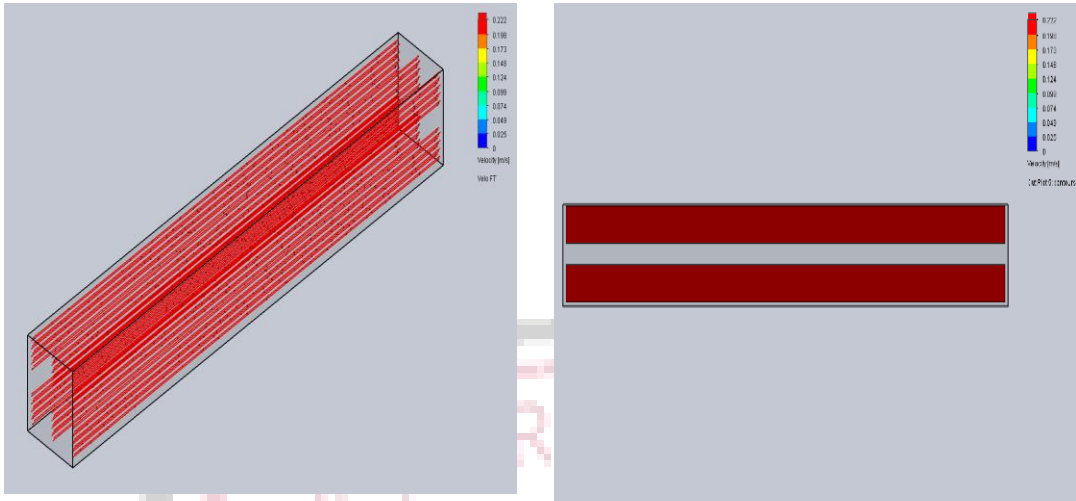


Figure 7 Velocity flow trajectory and cutplot along the radiator $m= 0.4 \text{ kg/s}$

Velocity flow trajectory and cut plot of radiator at $300 \text{ W/m}^2\text{.K}$

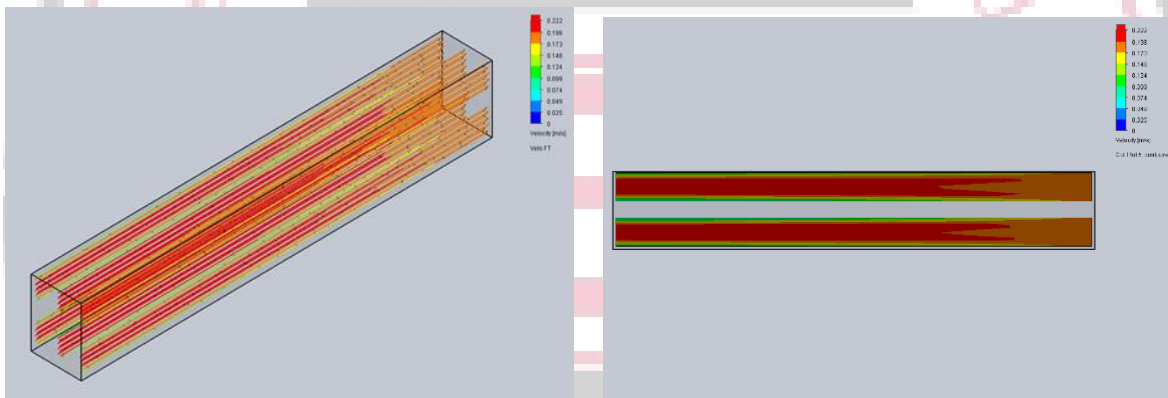


Figure 8 Velocity flow trajectory and cutplot along the radiator $m= 0.1 \text{ kg/s}$

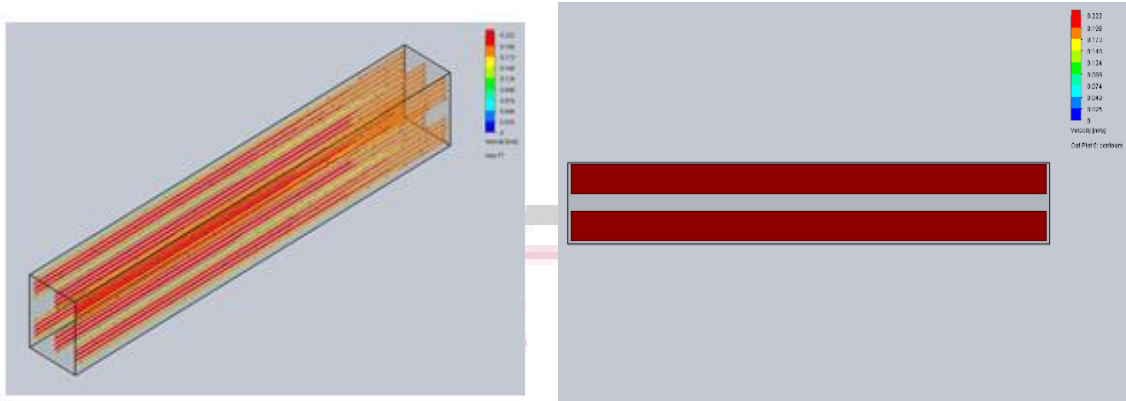


Figure 9 Velocity flow trajectory and cutplot along the radiator $m= 0.2 \text{ kg/s}$

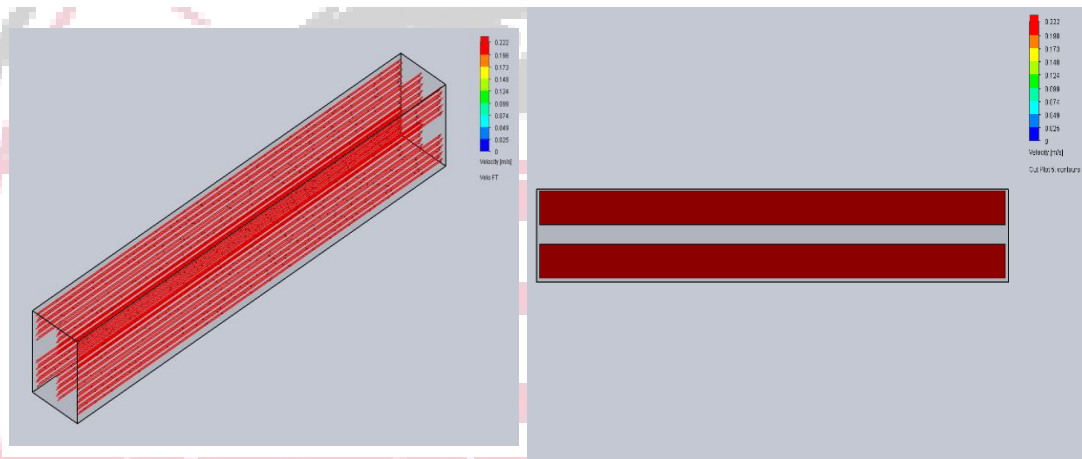


Figure 10 Velocity flow trajectory and cutplot along the radiator $m= 0.3 \text{ kg/s}$

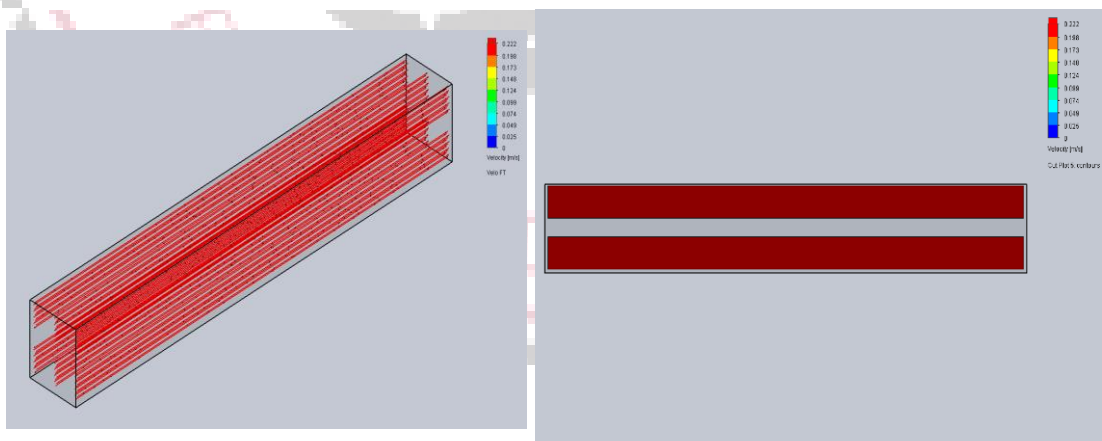


Figure 11 Velocity flow trajectory and cutplot along the radiator $m= 0.4 \text{ kg/s}$

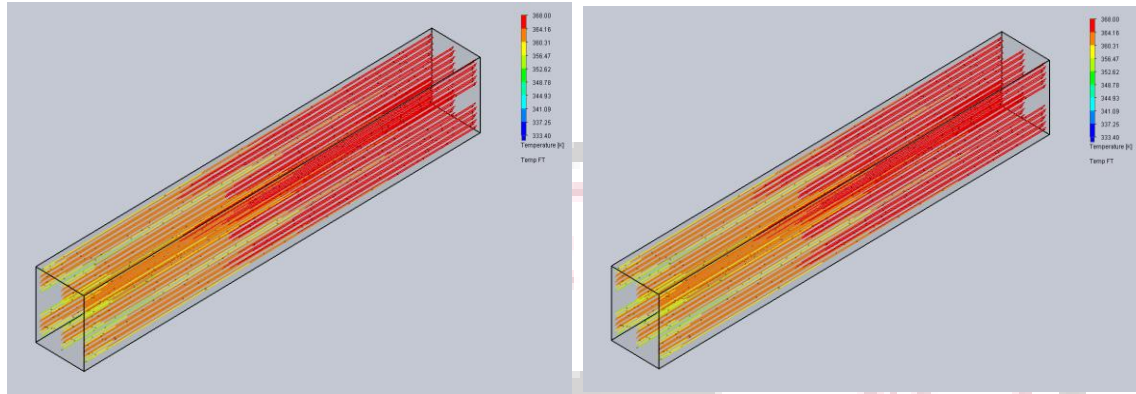


Figure 12 Temperature flow trajectory along the radiator $m= 0.1 \text{ kg/s}$

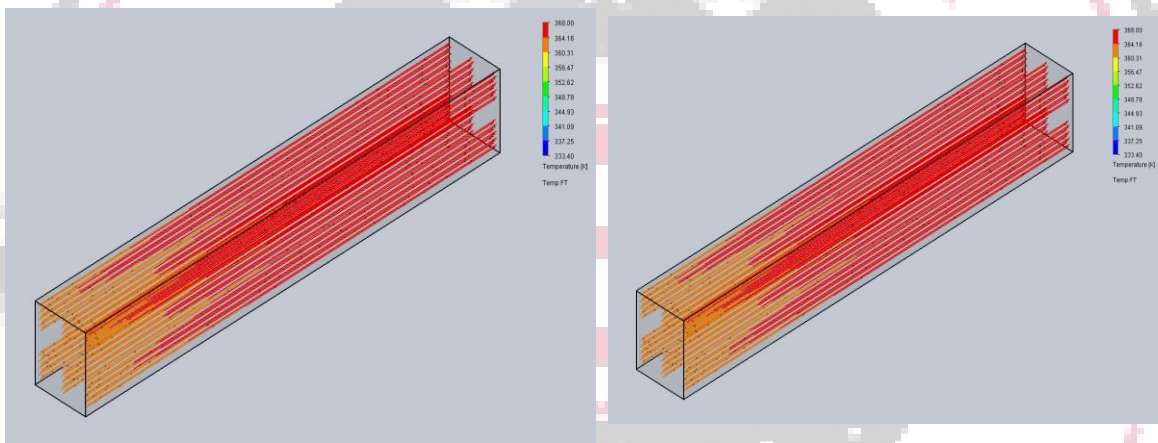


Figure 13 Temperature flow trajectory along the radiator $m= 0.2 \text{ kg/s}$

Temperature flow trajectory comparison of Radiator at 300 and 400 W/m².K

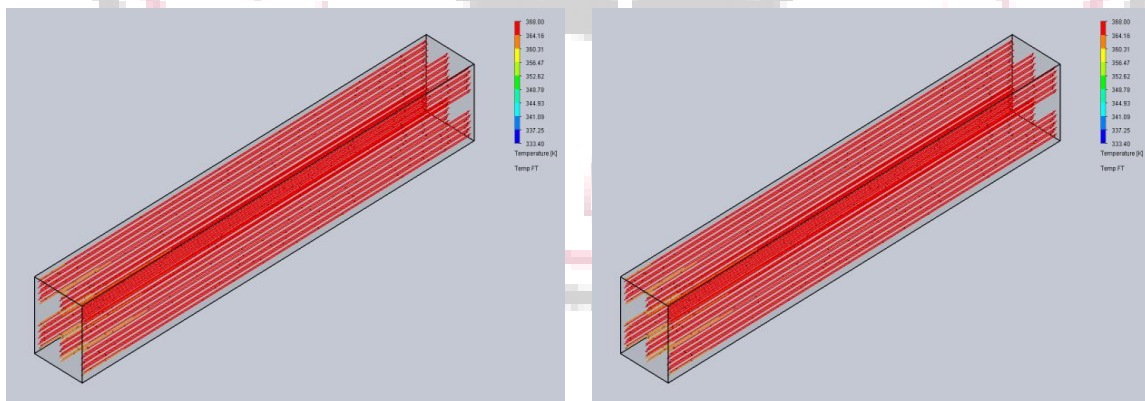


Figure 14 Temperature flow trajectory along the radiator $m= 0.3 \text{ kg/s}$

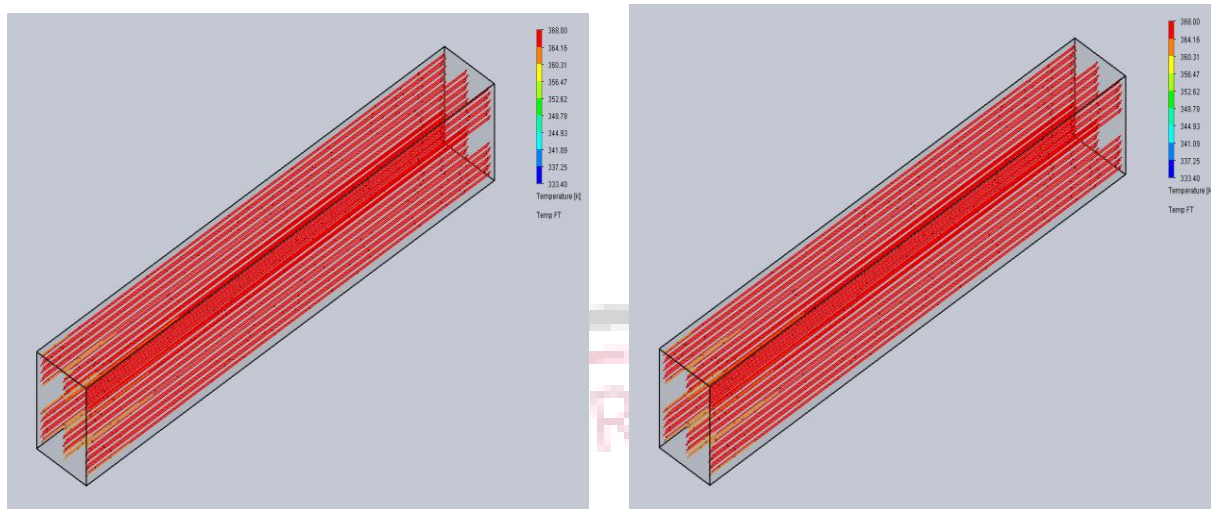


Figure 15 Temperature flow trajectory along the radiator $m= 0.4 \text{ kg/s}$

V.CONCLUSION

The study showed that the length of the fully developed velocity region decreases with an increase in mass flow rate and the flow is fully developed at the entrance of the tube at 0.3 Kg/s . The velocity profile has little significance on the heat transfer rate at 400 or $300 \text{ W/m}^2\text{K}$. The temperature profile of the radiator with honeycomb fins indicated that the length of the fully developed temperature region decreases with an increase in heat transfer coefficient. Moreover, temperature drop decreases with an increase in pressure drop for both heat transfer values. There is a small difference between pressure and temperature drops for the same value of heat transfer. The higher the flow rate, the lesser the temperature drop of the coolant due to less time for heat transfer from the coolant to fins, but this might increase if different cross-section tubes are used. Finally, flow in tubes is laminar due to the small cross-sectional area of the tubes, which indirectly decreases heat transfer.

REFERENCES

- [1] Abdulmunem, A. R., Samin, P. M., Rahman, H. A., Hussien, H. A., & Mazali, I. I. (2020). Enhancing PV Cell's electrical efficiency using phase change material with copper foam matrix and multi-walled carbon nanotubes as passive cooling method. *Renewable Energy*, 160, 663–675, ISSN 0960-1481. <https://doi.org/10.1016/j.renene.2020.07.037>
- [2] Xu, H., Wang, N., Zhang, C., Qu, Z., & Karimi, F. (2021). Energy conversion performance of a PV/T-PCM system under different thermal regulation strategies. *Energy Conversion and Management*, 229, 113660, ISSN 0196-8904. <https://doi.org/10.1016/j.enconman.2020.113660>
- [3] Wang, C. C. (2017). A quick overview of compact air-cooled heat sinks applicable for electronic cooling—Recent progress. *Inventions*, 2(1), 5. <https://doi.org/10.3390/inventions2010005>
- [4] Xu, H. J., Xing, Z. B., Wang, F. Q., & Cheng, Z. M. (2019). Review on heat conduction, heat convection, thermal radiation and phase change heat transfer of nanofluids in porous media: Fundamentals and applications. *Chemical Engineering Science*, 195, 462–483, ISSN 0009-2509. <https://doi.org/10.1016/j.ces.2018.09.045>
- [5] Zhao, D., & Li, L. (2015). Effect of choked outlet on transient energy growth analysis of a thermoacoustic system. *Applied Energy*, 160, 502–510, ISSN 0306-2619. <https://doi.org/10.1016/j.apenergy.2015.09.078>
- [6] Li, S., Wu, P., Cao, L., Wu, D., & She, Y. (2017). CFD simulation of dynamic characteristics of a solenoid valve for exhaust gas turbocharger system. *Applied Thermal Engineering*, 110, 213–222, ISSN 1359-4311. <https://doi.org/10.1016/j.applthermaleng.2016.08.155>
- [7] Zhao, D., Ji, C., Li, X., & Li, S. (2015). Mitigation of premixed flame-sustained thermoacoustic oscillations using an electrical heater. *International Journal of Heat and Mass Transfer*, 86, 309–318, ISSN 0017-9310. <https://doi.org/10.1016/j.ijheatmasstransfer.2015.03.012>
- [8] Wu, G., Wu, D., Li, Y., & Meng, L. (2020). Effect of acetone-n-butanol-ethanol (ABE) as an oxygenate on combustion, performance, and emission characteristics of a spark ignition engine. *Journal of Chemistry*, 2020, article ID 7468651. <https://doi.org/10.1155/2020/7468651>

- [9] Padzillah, M. H., Rajoo, S., & Martinez-Botas, R. F. (2014). Influence of speed and frequency towards the automotive turbocharger turbine performance under pulsating flow conditions. *Energy Conversion and Management*, 80, 416–428, ISSN 0196-8904. <https://doi.org/10.1016/j.enconman.2014.01.047>
- [10] E, J., Liu, G., Zhang, Z., Han, D., Chen, J., Wei, K., Gong, J., & Yin, Zibin. (2019). Effect analysis on cold starting performance enhancement of a diesel engine fueled with biodiesel fuel based on an improved thermodynamic model. *Applied Energy*, 243, 321–335, ISSN 0306-2619. <https://doi.org/10.1016/j.apenergy.2019.03.204>
- [11] J., Zuo, W., Gao, Junxu, Peng, Q., Zhang, Z., & Hieu, P. M. (2016). Effect analysis on pressure drop of the continuous regeneration-diesel particulate filter based on NO₂ assisted regeneration. *Applied Thermal Engineering*, 100, 356–366, ISSN 1359-4311. <https://doi.org/10.1016/j.applthermaleng.2016.02.031>
- [12] E, J., Zhang, Z., Chen, J., Pham, M.H., Zhao, X., Peng, Q., Zhang, B., & Yin, Zibin. (2018). Performance and emission evaluation of a marine diesel engine fueled by water biodiesel-diesel emulsion blends with a fuel additive of a cerium oxide nanoparticle. *Energy Conversion and Management*, 169, 194–205, ISSN 0196-8904. <https://doi.org/10.1016/j.enconman.2018.05.073>
- [13] Gonçalves, I., Souza, R., Coutinho, G., Miranda, J., Moita, A., Pereira, J. E., Moreira, A., & Lima, R. (2021). Thermal conductivity of nanofluids: A review on prediction models, controversies and challenges. *Applied Sciences*. MDPI, 11(6), 2525. <http://doi.org/10.3390/app11062525>
- [14] Sekrani, G., & Poncet, S. (2018). Ethylene- and propylene-glycol based nanofluids: A literature review on their thermophysical properties and thermal performances. *Applied Sciences*. MDPI, 8(11), 2311. <http://doi.org/10.3390/app8112311>
- [15] Pang, S. C., Kalam, M. A., Masjuki, H. H., & Hazrat, M. A. (2012). A review on air flow and coolant flow circuit in vehicles' cooling system. *International Journal of Heat and Mass Transfer*, 55(23–24), 6295–6306, ISSN 0017-9310. <https://doi.org/10.1016/j.ijheatmasstransfer.2012.07.002>

